Magazine of Civil Engineering

ISSN 2712-8172

journal homepage: http://engstroy.spbstu.ru/

Research article

UDC 625

DOI: 10.34910/MCE.112.5

Asphalt pavement rutting model in seasonal frozen area

L.N. Zhang[a], ***D.P. He***[a] ✉, ***Q.Q. Zhao***[b]

[a] *Northeast Forestry University, Harbin, Heilongjiang, China*

[b] *Northeast Agricultural University, Harbin City, Heilongjiang Province, China*

✉ *hdp@nefu.edu.cn*

Keywords: deterioration, pavement maintenance, design model

Abstract. Effective prediction of rutting diseases in seasonal frozen area is helpful for comprehensive evaluation of asphalt pavement performance. In this paper, based on the Mechanical-Experienced Pavement Design Guide (MEPDG) theory, the rutting prediction model of asphalt pavement in the seasonal frozen area is established by using the measured rutting data of 9 typical highways in the seasonal frozen area of China. The research results show that the traffic volume, climate, and asphalt layer thickness of the pavement structure are directly proportional to the change in rutting. The proposed correction coefficients for the prediction model of asphalt pavement rutting in the seasonal frozen area are $\beta_{1r} = 2$, $\beta_{2r} = 1.03$ and $\beta_{3r} = 0.93$. The normal distribution map and P-P map of the rutting prediction model conform to the normal distribution. The fit between the predicted data of the prediction model and the measured data is high. The fitting value between the predicted data and the measured data before correction is $R^2 = 0.9357$. The fitting value between the revised predicted data and the measured data is $R^2 = 0.9925$. The research results are of great significance for the prediction of rutting and maintenance of asphalt pavement in the seasonal frozen area.

Citation: Zhang, L.N., He, D.P., Zhao, Q.Q. Asphalt pavement rutting model in seasonal frozen area. Magazine of Civil Engineering. 2022. 112(4). Article No. 11205. DOI: 10.34910/MCE.112.5

1. Introduction

With the rapid development of heavy-duty transportation, rutting disease has become the most important form of damage to asphalt pavement. The climate characteristics of the seasonal frozen area are the huge temperature difference between winter and summer, and the freeze-thaw cycle repeating many times in spring and autumn, which will further aggravate the rutting problem of asphalt pavement in the seasonal frozen area of China. Therefore, it is very important to accurately predict the rutting value. Research scholars at home and abroad have proposed a variety of rutting prediction methods for different highway grades. R. Tarefder et al. [1] conducted a local calibration of the Mechanical-Experienced Pavement Design Guide (MEPDG) lines, and the calibrated model can eliminate the prediction deviation of rutting and improve the accuracy of prediction accuracy. Z. Wu et al. [2] Used the design software (MEPDG), the PCC performance of Portland cement concrete (PCC) and asphalt mixture overlay on an unbonded base was analyzed by comparing the evaluation performance of a typical Louisiana rigid pavement structure. A new design method is proposed. M. Mubaraki [3] selected and analyzed to investigate the relationship between International Roughness Index (IRI) and pavement damage including cracking, rutting, and raveling; J. Saha et al. [4] analyzed the sensitivity of the influence of total climate road rutting and international roughness index; W.S. Mogawer et al. [5] used the Mechanical-Empirical Pavement Design Guide (MEPDG) damage prediction equation to predict the mixture performance as a function of density, which only aimed at the influence of hot mix asphalt mixture fatigue crack and rutting

performance; Gulfam-E-Jannat, X.X. Yuan [6] could predict IRI and rutting depth for calibration, but the applicability of the model is only for Ontario in the United States.

Rutting will lead to poor smoothness of the pavement, reduce the performance of the pavement, affect the service life of the pavement and even endanger traffic safety. In the seasonal frozen area, the accurate prediction of rutting can effectively improve the performance of the pavement, thereby extending the service life of the highway. Based on the continuous rutting observation data of typical highways in the seasonal frozen area of China, and based on MEPDG theory, this paper establishes a rutting prediction model of asphalt pavement in the seasonal frozen area, so as to predict the rutting depth of asphalt pavement more accurately. Accurate prediction of rutting depth can take effective control measures for asphalt pavement rutting, thereby improving the highway performance in the seasonal frozen area and extending the service life of highways, providing a maintenance reference for asphalt pavement. Therefore, this study has very important practical significance, social and economic benefits.

2. Methods

2.1. MEPDG rutting prediction model

Through the observation, investigation and arrangement of the long-term road performance of more than 2200 test roads in various states of the United States, American Association of State Highway and Transportation Officials (AASHTO), the and the National Cooperative Highway Research Project, (NCHRP), launched the Mechanistic-Empirical Pavement Design Guide, MEPDG [7–15], which is suitable for local climatic conditions in the United States in 2004. MEPDG's prediction model of asphalt pavement rutting, such as formula (1)-(4):

$$\Delta p\left(HMA\right)=\varepsilon_{p(HMA)}h_{HMA}=\beta_{1\gamma}k_Z\varepsilon_{\gamma(HMA)}10^{k_{1\gamma}}n^{k_{2\gamma}\beta_{2\gamma}}T^{k_{3\gamma}\beta_{3\gamma}}, \quad (1)$$

$$k_Z=\left(C_1+C_2D\right)0.328196D, \quad (2)$$

$$C_1=-0.1039\left(H_{HMA}\right)^2+2.4868H_{HMA}-17.342, \quad (3)$$

$$C_2=0.0172\left(H_{HMA}\right)^2-1.7331H_{HMA}+27.428, \quad (4)$$

where $\Delta p\left(HMA\right)$ is accumulated permanent or plastic vertical deformation in the HMA layer/sublayer, in., $\varepsilon_{p(HMA)}$ is accumulated permanent or plastic axial strain in the HMA layer/sublayer, in/in., h_{HMA} is thickness of the HMA layer/sublayer, in., k_Z is depth confinement factor, $\varepsilon_{\gamma(HMA)}$ is resilient or elastic strain calculated by the structural response model at the mid-depth of each HMA sublayer, in/in., $k_{1\gamma}$, $k_{2\gamma}$, $k_{3\gamma}$ are global field calibration parameters (from the NCHRP 1-40D recalibration; $k_{1\gamma}=-3.35412$, $k_{2\gamma}=0.4791$, $k_{3\gamma}=1.5606$), and $\beta_{1\gamma}$, $\beta_{2\gamma}$, $\beta_{3\gamma}$ are local or mixture field calibration constants; for the global calibration, these constants were all set to 1.0., n is number of axle-load repetitions, T is mix or pavement temperature, °F, D is depth below the surface, in., and H_{HMA} is total HMA thickness, in.

Through the model [16–21], it can be judged that traffic volume, climate condition and pavement structure are important parameters that affect the rutting of asphalt pavement. Therefore, in order to put forward the rutting prediction model of asphalt pavement in the seasonal frozen area, it is necessary to verify whether there is a correlation between rutting and n, T, H_{HMA}.

2.2. Analysis of parameters affecting rutting performance

In order to reflect the climatic characteristics of the seasonal frozen area, nine typical highways are selected to fully cover the climatic conditions of the seasonal frozen area in China. The names and geographical locations of all typical highways are shown in Fig. 1. The selected typical highway has a great difference in longitude and latitude, which can more fully reflect the climatic characteristics of the seasonal frozen area in China. In order to reflect the climatic characteristics of the seasonal frozen area, 6 typical highways were selected in Northeast China.

Figure 1. Geographic location of typical highways.

2.2.1 Traffic load parameters

In order to verify whether there is a correlation between rutting and climate in the seasonal frozen area, Jian-Ji Highway and Jian-Hei Highway are selected for comparison. The pavement structure parameters and climate parameters of the two highways are similar, but there are significant differences in traffic volume. Compare the uplink and downlink traffic volume of the K45+000~K91+495 section of Jian-Ji Highway and the K168+485~K217+905 section of Jian-Hei Highway, as shown in Fig. 2, and the data in the figure shows the comparison of the total number of vehicles on the two roads in 2018. The total number of uplink vehicles in Jian-Ji Highway is 9623, of which 3410 are heavy trucks, and the total number of downlink vehicles is 9752, of which 3464 are heavy trucks. The total number of uplink vehicles in Jian-Hei Highway is 7896, of which 2784 are heavy trucks, and the total number of downlink vehicles is 9047, of which 3154 are heavy trucks. The total number of vehicles can not see the damage to the actual road surface caused by the traffic volume, because the impact of extra heavy vehicles on the road surface far exceeds the general axle load. Therefore, by comparing the axle load distribution of several observation sections with similar number of vehicles, the traffic parameters of several observation sections can be reflected in more detail. The American Standard 9 and 10 cars passed by each observation section are taken as the research object, because these two kinds of vehicles cover most of the double-axle and all three-axle models.

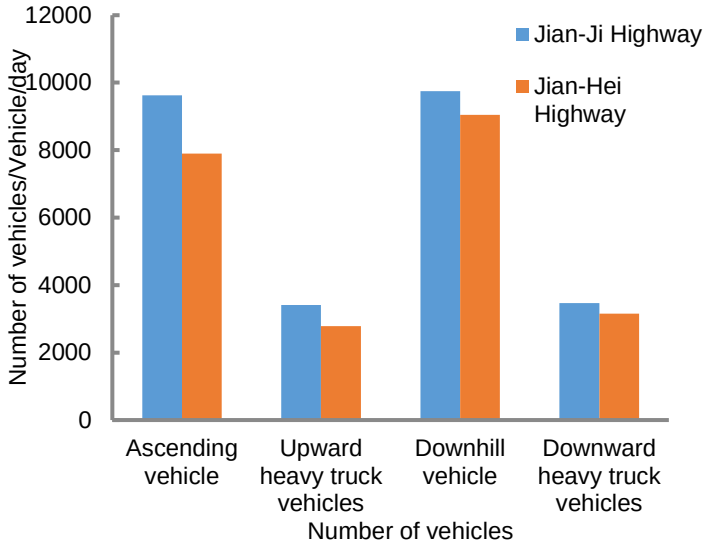

Figure 2. Comparison of the number of vehicles and heavy vehicles in different road sections.

The axle load distribution is shown in Fig. 3 and 4. It can be seen from the figure that the axle load of Jian-Ji Highway is obviously larger than that of Jian-Hei Highway, and the asphalt pavement of Jian-Ji Highway bears heavier traffic load.

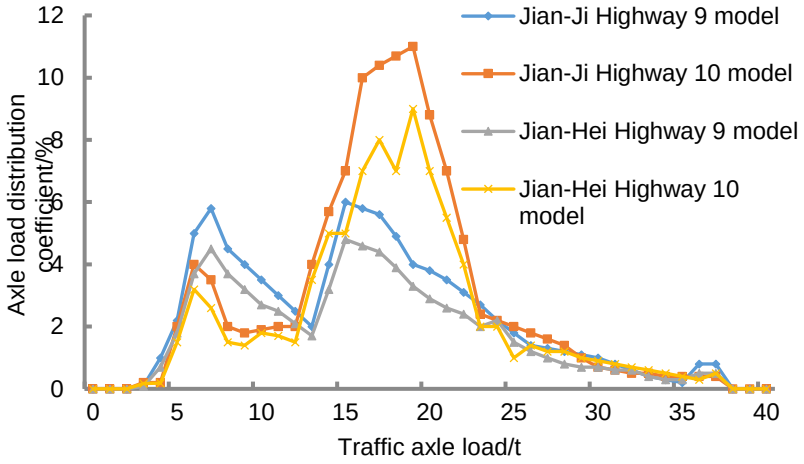

Figure 3. Comparison of axle load distribution of double couplings of overweight vehicles in different road sections.

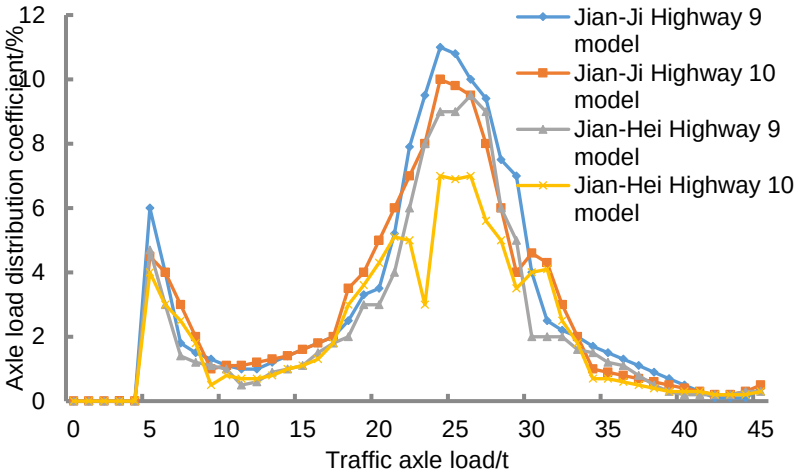

Figure 4. Comparison of axle load distribution of triple axles of overweight vehicles in different road sections.

Between 2014 and 2018, the growth rate of Jian-Ji Highway's rutting value was 33.4 %. The growth rate of Jian-Hei Highway was 26.6 %, with an average annual growth rate of 8.35 % and 6.65 %, respectively, as shown in Fig. 5. According to the analysis of the reasons, both Jian-Ji Highway and Jian-Hei Highway are located in Heilongjiang Province, China. The climate temperature of the two highways is similar and the pavement structure is the same, but the large traffic volume of Jian-Ji Highway leads to a faster increase in rutting value.

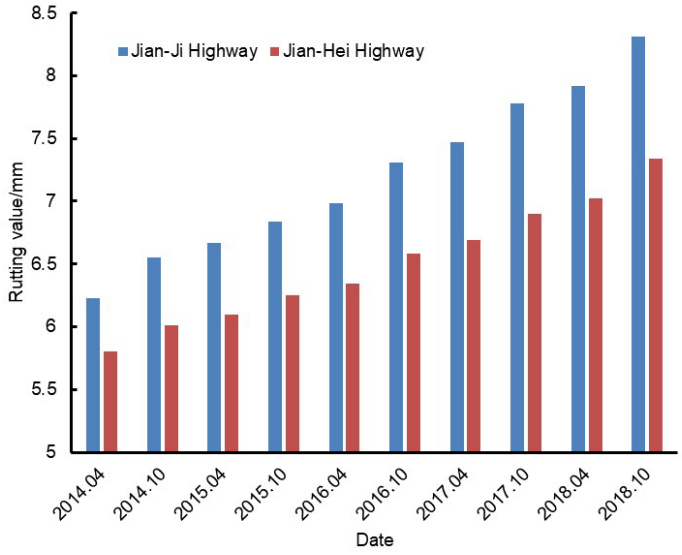

Figure 5. Comparison of rutting values between Jian-Ji Highway and Jian-Hei Highway.

2.2.2 Climatic parameters

In order to verify whether there is a correlation between rutting and climate in the seasonal frozen area, the influence on rutting is verified by selecting air temperature, average annual freezing index and average annual precipitation from the climatic conditions. The monthly mean temperature curve, freezing depth curve and precipitation distribution curve corresponding to four typical highways such as Jian-Ji Highway (Yanggang to Mishan Section), Zhang-Shi Highway (Zhangjiakou Section), Lian-Huo National Highway (Kuitun-Wusu Section) and 110 National Highway (Hubao section) are drawn respectively, as shown in Fig. 6–8.

As the temperature in the seasonal frozen area is lower than 0 °C, from October to March of the following year, the time for a complete freeze-thaw process is set from October of 2017 to October of 2018. The influence of temperature on asphalt pavement is compared and analyzed. As can be seen from Fig. 6, there is a gap in the monthly average temperature of the cities where the four highways are located. The month with the largest temperature difference is February 2018. The monthly mean temperature difference between Jian-Ji Highway and Zhang-Shi Highway cities is 10 °C, and the air temperature difference is 3 times. Among the four typical highways, Lian-Huo National Highway has the lowest temperature in winter. The average temperature in January 2018 is –18 °C, and the temperature in summer is the highest. The average temperature in July 2018 is 27.5 °C, which is the year-round among the four typical highways. The road with the largest temperature difference has a temperature difference of 45.5 °C throughout the year. Zhang-Shi Highway has the smallest temperature difference throughout the year. The monthly minimum temperature of the four typical highways appeared in January 2018. The monthly average temperature difference between Lian-Huo National Highway and Zhang-Shi Highway is 9 °C, and the difference in temperature value is 2 times. The highest monthly average temperature occurred in July 2018. The monthly average temperature difference between Lian-Huo National Highway and 110 National Highway is 4.5 °C, and the difference in temperature value is 0.83 times.

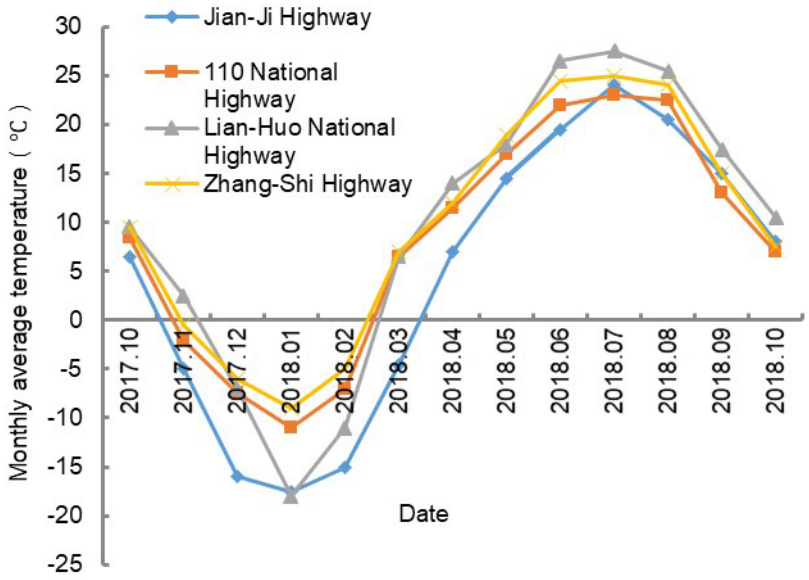

Figure 6. Change of monthly mean temperature curve.

Fig. 7 shows the precipitation distribution curve of four typical highways from January to December 2018. The season with the highest rainfall on the four highways occurs in July, in which Jian-ji Highway is the largest and Lian-Huo National Highway is the smallest. The month in which the maximum precipitation occurs is also in line with the actual characteristics of climatic precipitation in the seasonal frozen area. The highway with the largest annual precipitation is Jian-Ji Highway, with an annual precipitation of 407 mm, accounting for 5.28 %, 24.69 %, 62.04 % and 7.99 % of the annual precipitation in spring, summer, autumn and winter, respectively. The precipitation of Zhang-Shi Highway is 397.3 mm, and spring, summer, autumn and winter account for 4.3 %, 30.4 %, 58.07 % and 7.22 % of the annual precipitation, respectively. The precipitation of Lian-huo National Highway is 175.5 mm, accounting for 12.82 %, 39.66 %, 28.72 % and 18.8 % of the annual precipitation, respectively. The precipitation of 110 National Highway is 402.3 mm, and spring, summer, autumn and winter account for 5.1 %, 25.98 %, 59.98 % and 8.93 % of the annual precipitation, respectively. As can be seen from Fig. 7, January to March 2018 and October to December of 2018 are the periods when the precipitation of the four typical highways is relatively less, which is due to the fact that the four highways have entered winter one after another.

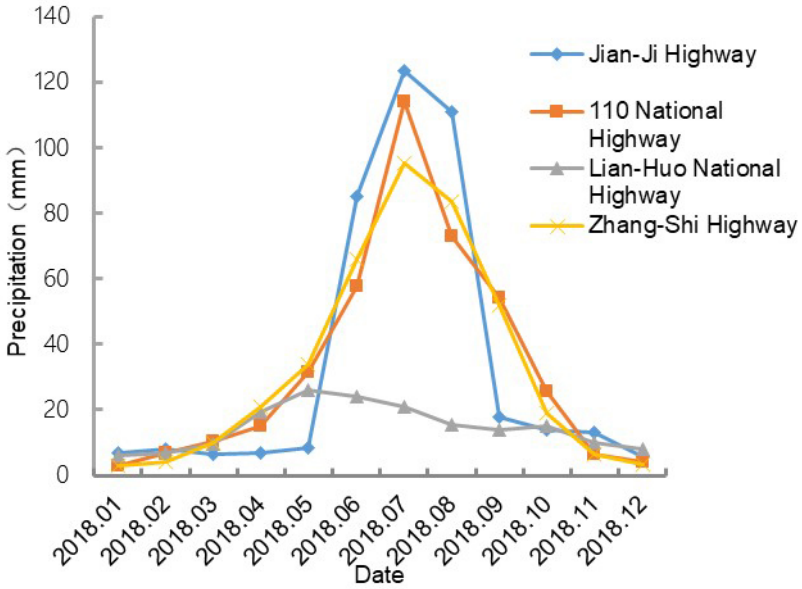

Figure 7. Precipitation distribution curve.

Fig. 8 shows the freezing depth curves of four typical highways. Since the freezing time of roads in the seasonal frozen area is from October to April of the following year, the freezing depth values of the four curves are basically 0 cm from May 2018 to September 2018. The maximum freezing depth of the four typical highways appeared in February 2018. Among them, the maximum freezing depth of Jian-Ji Highway, in northeastern China was 217 cm, followed by Lian-Huo National Highway, in northwestern China, 164 cm. The third is 110 National Highway in northern China, whose maximum deep value is 152 cm. The sminimum freezing depth is Zhang-Shi Highway, whose maximum freezing depth is 110 cm. The difference between the maximum freezing depth and the minimum freezing depth is 107 cm. The reason is that in February 2018, the temperature difference between Jian-Ji Highway and Zhang-Shi Highway is 3 times, and the precipitation difference is 1.95 times. Under the coupling action of precipitation and temperature, the difference in freezing depth is significant.

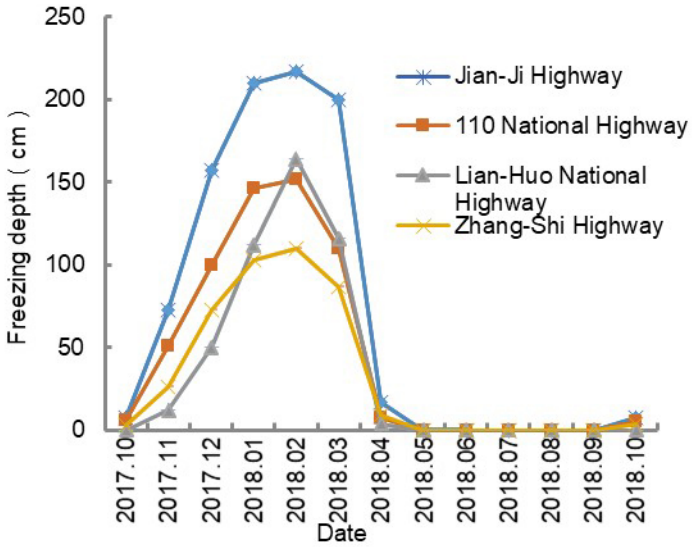

Figure 8. Freezing depth curve.

In order to further analyze the influence of climatic factors on the rut disease of asphalt pavement, the rutting depth curves of four highways from 2014 to 2018 are established, as shown in Fig. 9. In Fig. 9, the rutting values of the four highways change with time, and the change law is linear growth. For example, the rutting depth of Zhang-Shi highway increased by 0.29 mm in October 2014 compared with April 2014, and 0.13 mm in April 2015 compared with October 2014. The rutting depth of the same highway in October every year is greater than that in April. According to the analysis of the reasons, the temperature began to rise in April, the highway in the seasonal frozen area began to thaw, and the rutting disease of the pavement developed rapidly under the repeated action of external loads. The rutting depth in October has experienced many times of freezing and thawing in spring and hot high temperature in summer, so the rutting depth measured in October varies greatly. From April 2014 to April 2018, the change rate of

Lian-Huo Highway rutting depth is 59.5 %, which is the largest among the four highways, followed by 110 National Highway, whose rut depth change rate is 35.3 %. The third is Jian-Ji Highway, whose rutting depth change rate is 33.3 %. The slowest development of rutting disease is Zhang-Shi Highway, whose rutting depth change rate is 30.8 %. According to the analysis of the reasons, the freezing depth and rainfall of the highway in the seasonal frozen area are not the decisive factors affecting the rutting value, but the air temperature is the main factor affecting the rutting disease of the highway in the seasonal frozen area. The higher the temperature is, the faster the rutting disease develops.

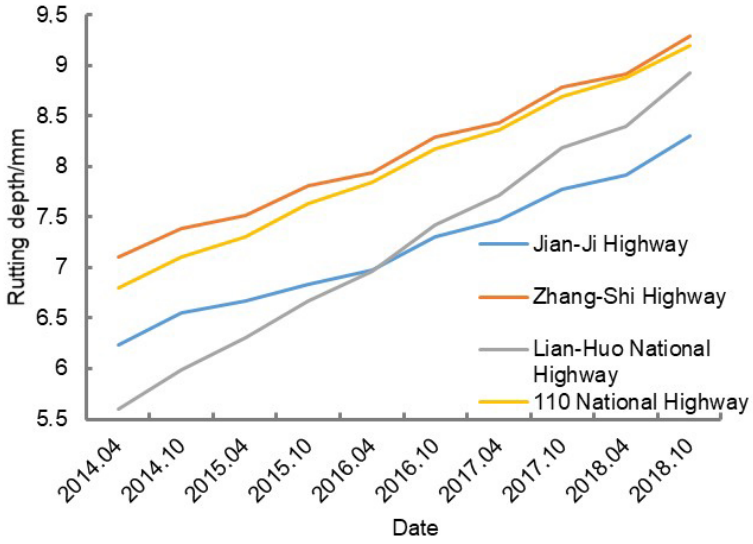

Figure 9. Rutting depth variation curve.

2.2.3 Analysis of pavement structure parameters

In order to verify whether the correlation between rutting and H_{HMA} accur in the seasonal frozen area, four highways with similar traffic volume and climatic conditions but different asphalt thickness of pavement structure are selected: Hei-Da Highway, Sui-Man Highway, Qi-Zha Highway, and Jia-Lin Highway. The effects of asphalt thickness of different pavement structures on rutting are compared. The proportion of rutting on the four highways is compared in Fig. 10. According to the analysis of Fig. 10, the thickness of the asphalt layer of Hei-Da Highway is the largest, which is 240 mm. The rutting disease of the highway develops most rapidly, and the rutting depth is concentrated between 5~12 mm, in which the rutting depth of 5~8 mm is 39 %, and the rutting ratio of 8 mm to 12 mm is 38 %. The thickness of the asphalt layer of Sui-Man Highway is 180 mm and the rutting ratio of 5 mm to 8 mm is 35 % to that of 8~12 mm. The asphalt layer thickness of Qi-Zha Highway is 150 mm, the proportion of rutting is 31 %, and the proportion of rutting of 8~12 mm is 32 %. The asphalt layer thickness of Jia-Lin Highway is 120 mm, the rutting ratio of 5~8 mm is 26 %, and the rutting ratio of 8~12 mm is 31 mm. For the typical highway in the seasonal frozen area, the transverse crack is one of the main disease characteristics of the asphalt pavement. The thicker the asphalt layer of the asphalt pavement is, the faster the rutting disease develops.

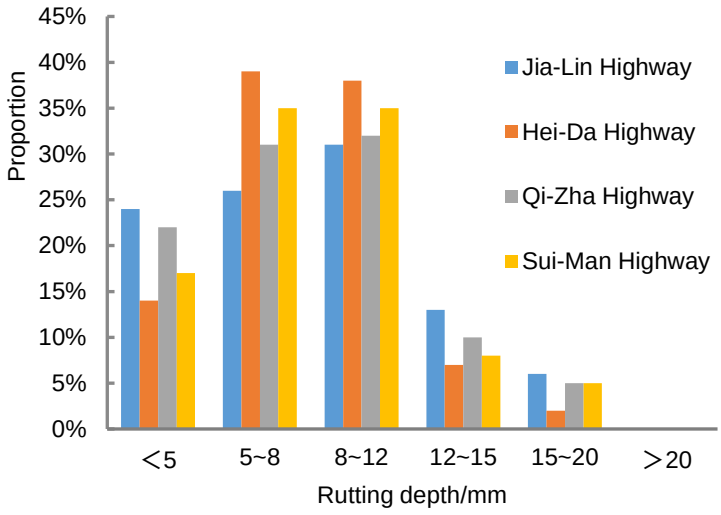

Figure 10. Rutting ratio of four highways.

From the above analysis of the rutting value of the asphalt pavement, the disease of the asphalt pavement in the seasonal frozen area is mainly rutting, and the rutting value increases with the increase of the thickness of the pavement structure when the climate condition and traffic volume are basically the same. And the development form is mainly transverse temperature shrinkage cracks.

2.3. Processing of measured rutting data

In order to establish a rutting prediction model suitable for asphalt pavement in seasonal frozen area, the rutting values of typical highways in seasonal frozen area are measured in situ. The measured time is from 2014 to 2018. The rutting values of 9 typical highways in the seasonal frozen area of China are collected by road multi-function monitoring vehicles and calibrated manually. They are measured and calibrated four times a year, and 10m per lane is measured once. In this paper, the lane with the largest rutting value is used for data analysis.

MEPDG rutting prediction model uses 90 % design reliability to calculate rutting, so the measured rutting data of typical highways are processed based on normal distribution, and the measured rutting data of corresponding 90 % frequency ratio are used. The measured rutting values of different stations should be random variables that meet the normal distribution, which ensures the rationality of the selected data.

3. Results and Discussion

3.1. Construction of rutting prediction model based on MEPDG theory

The advantage of the rutting prediction model proposed by MEPDG theory is that the factors considered in the calculation process are more comprehensive, which can reflect the actual use of the pavement more closely, and has higher accuracy. However, because the rutting prediction model proposed by MEPDG theory is based on the climatic conditions of the United States and the measured data of thousands of local test sections, the model has regional limitations. Therefore, this paper intends to modify the rutting prediction model of asphalt pavement in the seasonal frozen area according to the climatic conditions of the seasonal frozen area in China and the measured rutting values of 9 typical highways.

In the process of modifying the MEPDG rutting prediction model, firstly, the default local correction coefficient of the system, that is, $\beta_{1r}=\beta_{2r}=\beta_{3r}=1$, is adopted, from which the formula (5) is obtained:

$$\Delta p\left(HMA\right)=\varepsilon_{p(HMA)}h_{HMA}=k_Z\varepsilon_{\gamma(HMA)}10^{-3.35412}n^{0.4791}T^{1.5606}h_{HMA}. \quad (5)$$

In the formula, Δp_H is the predicted value of rutting after correction, and n is the number of repeated loads, which is obtained by equivalent conversion of axle load spectrum.

By dividing (1) by (5), a relationship (6) before and after the correction of MEPDG rutting prediction model can be obtained, that is:

$$\Delta p_H/\Delta p_Q=\beta_{1\gamma}n^{0.4791\left(\beta_{2\gamma}-1\right)}T^{1.5606\left(\beta_{3\gamma}-1\right)}. \quad (6)$$

In the formula, Δp_Q, Δp_H are the predicted values of rut before and after correction, n is the number of repeated loads, which is obtained by indoor repeated loading triaxial permanent deformation test, and T is the road surface temperature (°F), which is the average value of the annual maximum temperature in the seasonal frozen area of China in the past 10 years.

Formula (6) is used as the relation function in the solution of Excel programming. By using the function of "data analysis" in Excel programming solving method, the nonlinear model can be transformed into linear model, and the transformed multivariate nonlinear model can be analyzed by regression and verify its validity and feasibility. Based on the rut measurement data of 9 highways above, the rutting prediction model of the seasonal frozen area based on MEPDG theory is established. Some of the operation data are shown in Table 1. In the process of creating the model, use Excel Solver to establish constraint conditions for the variable cell values in the Solver model. The constraint conditions are formulas 1-4. By changing the MEPDG rut value before correction, the rut prediction after correction is determined.

The three values of local correction coefficients are calculated based on the rut prediction value before correction and the rut prediction value after correction. Because all the calculation data are calculated based on the road detection data in the seasonal frozen area, according to formula 1-4. Using matlab to perform background calculations and solutions. Therefore, it is concluded that the three

coefficients are local correction coefficients. In order to verify that their calculations are accurate, they are tested by the sum of squared errors (SSE). SSE is the sum of squared deviations within the group, which is used to test errors caused by errors. The value of the squared error in the article is only 3.89641, which is very small, which proves that the local correction coefficient obtained is accurate.

$$SSE = \sum_{i=1}^{k} \sum_{j=1}^{n_i} \left(x_{ij} - \overline{x_i} \right)^2 . \tag{7}$$

In the formula, SSE is the sum of squared deviations within the group, which is the variation caused by sampling error; k is the level number of the control variable; x_{ij} is the j-th sample value under the i-th level of the control variable; n_i is the control variable The sample size at the i-th level; $\overline{x_i}$ is the sample mean of the observed variable at the i-th level of the control variable.

Table 1. Determination of coefficients of rutting prediction model based on MEPDG theory according to planning solution. (The measured data of rutting of typical highways in the seasonal frozen area of China).

Serial number	Measured value of rutting/mm	MEPDG rutting prediction value / mm		Local correction coefficient	Target value (Sum of squares of errors)
		Before correction	After correction		
1	8.1	7.7	8.0	2.00	3.89641
2	4.2	4.5	4.1	1.03	
3	5.4	5.8	5.2	0.93	
4	7.1	7.6	7.0		
5	4.3	4.7	4.2		
6	7.5	7.0	7.4		
7	6.3	6.0	6.2		
8	6.1	6.5	5.9		
9	5.8	5.4	5.7		
10	6.3	6.6	6.2		
11	7.7	8.1	7.6		
12	5.2	5.7	5.1		
13	8.1	8.5	8.0		
14	7.6	7.3	7.5		
15	6.9	7.2	6.7		
16	…	…	…		

It can be seen from Table 1 that the correction coefficients of the seasonal frozen area of MEPDG rutting prediction model obtained by using planning solution method are $\beta_{1r} = 2,\ \beta_{2r} = 1.03,\ \beta_{3r} = 0.93.$ The modified seasonal frozen area correction coefficient is brought into the formula (1), and the modified MEPDG rutting prediction model is obtained as the formula (8):

$$\begin{aligned} \Delta p\left(HMA\right) &= \varepsilon_{p(HMA)} h_{HMA} = \\ &= 2k_Z \varepsilon_{\gamma(HMA)} 10^{-3.35412} n^{0.49235985} T^{1.45366232} h_{HMA}. \end{aligned} \tag{8}$$

3.2. Model verification

The measured data of asphalt pavement rutting are fitted with the rutting prediction value based on MEPDG theory, and the normal distribution map and P-P diagram are used to verify whether the model has universal applicability in statistics. The distribution of the difference (residual) between the measured value and the measured value of the MEPDG rutting prediction model is normally distributed as shown in Fig. 11. It is always assumed that the residual is consistent with the normal distribution in the process of regression using SPSS [22]. From the histogram and normal curve distribution of the regression residual of Fig. 11(a), we can see that the sample size is large enough and the residual distribution obviously obeys

the normal distribution. This shows that the regression prediction model has universal applicability in statistics, and there is no autocorrelation and multiple collinearity among variables, so it proves the accuracy of MEPDG rutting prediction model. Fig. 11(b) is the P-P diagram of the regression normalized residual of the rutting prediction model, and the residual P-P diagram between the cumulative probability of the actual measured value and the cumulative probability of the expected estimated result. It can be seen from Fig. 11(b) that the distribution curve of the residual is distributed around the specified straight line and changes around the straight line, indicating that the distribution of the residual P-P diagram can satisfy the pre-set normal distribution and the equation has practical significance. To sum up, the MEPDG rutting prediction model has passed various tests, and the fitting effect is well.

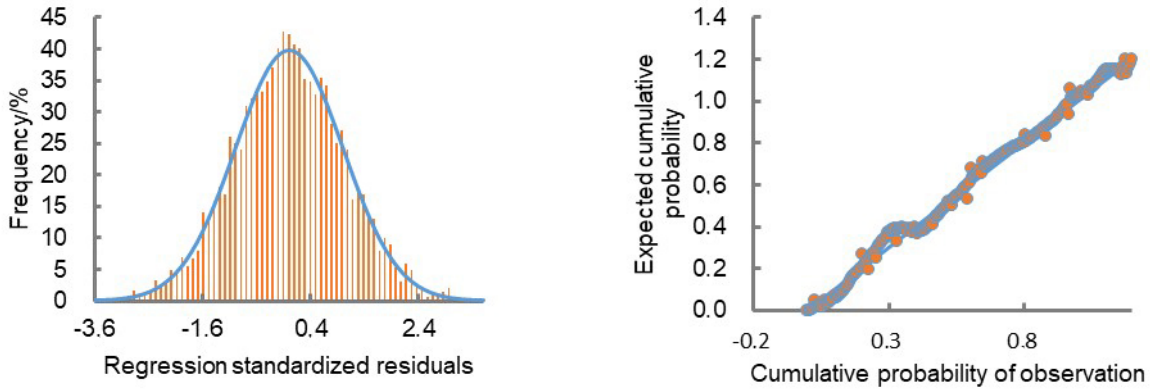

(a) Residual histogram **(b) Residual regression PMI P diagram**

Figure 11. Rutting prediction residual histogram and residual regression P-P chart.

The modified results of the rutting prediction model based on MEPDG theory [23–27] are fitted and verified, as shown in Fig. 12. Fig. 12(a), the result before correction represents the prediction result based on MEPDG theory. Fig. 12(b), the revised result is the prediction result of this revised model. It can be seen from Fig. 12 that the fitting coefficient between the predicted rutting value of MEPDG before correction and the measured value of rutting over the years is R^2 = 0.9357, and the fitting coefficient between the predicted value of modified MEPDG and the measured value is R^2 = 0.9925. It can be concluded that the modified MEPDG rutting prediction model has higher accuracy.

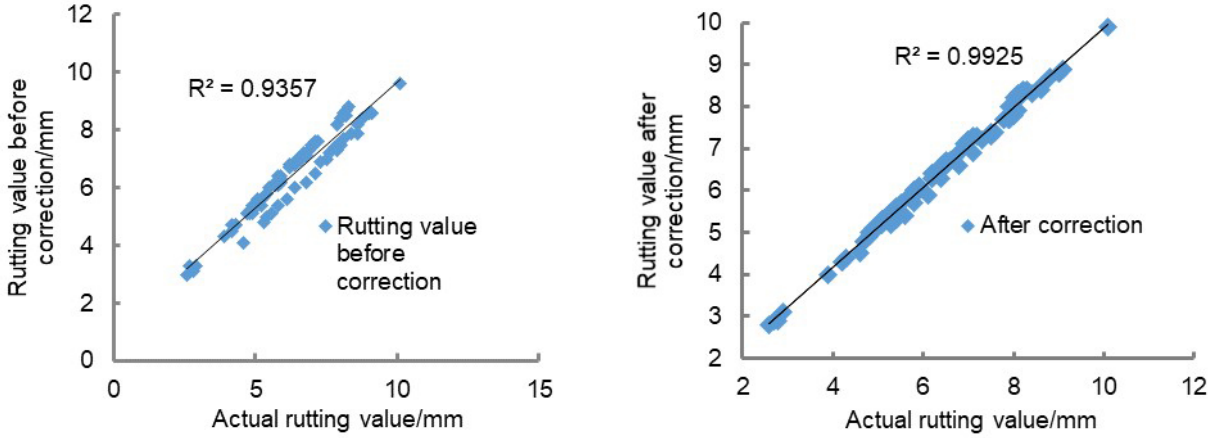

(a) Before correction **(b) After correction**

Figure 12. Correction effect of MEPDG rutting prediction model.

4. Conclusion

1. The traffic volume, climate and the thickness of asphalt layer of pavement structure are the key factors that affect the rutting change in the seasonal frozen area, and they are proportional to each other.

2. A rutting prediction model for asphalt pavement in the seasonal frozen area is proposed. Among them, β is the correction coefficient of the seasonal frozen area, and the modified coefficients are $\beta_{1r} = 2$, $\beta_{2r} = 1.03$, $\beta_{3r} = 0.93$, respectively.

3. The normal distribution map and P-P map of the rutting prediction model accord with the normal distribution, which is generally applicable in statistics.

4. The prediction accuracy of rutting prediction model is higher. The fitting value between the predicted data and the measured data before correction is obtained, and the fitting value between the modified predicted data and the measured data is R^2 = 0.9357, and the fitting value between the modified predicted data and the measured data is R^2 = 0.9925. This shows that there is a higher degree of fit between the revised predicted data and the measured data.

References

1. Tarefder, R., Rodriguez-Ruiz, J.I. Local calibration of MEPDG for flexible pavements in New Mexico. Journal of Transportation Engineering. 2013. 139(10). Pp. 981–991. DOI: 10.1061/(ASCE)TE.1943-5436.0000576
2. Wu, Z., Xiao, D.X., Zhang, Z., Temple, W.H. Evaluation of AASHTO Mechanistic-Empirical Pavement Design Guide for designing rigid pavements in louisiana. International Journal of Pavement Research and Technology. 2014. 7(6). Pp. 405–416. DOI: 10.6135/ijprt.org.tw/2014.7(6).405
3. Mubaraki, M. Highway subsurface assessment using pavement surface distress and roughness data. 8th International Conference on Maintenance and Rehabilitation of Pavements, MAIREPAV 2016. 9(5). Pp. 393–402. DOI: 10.3850/978-981-11-0449-7-329-cd
4. Saha, J., Nassiri, S., Bayat, A., Soleymani, H. Evaluation of the effects of Canadian climate conditions on the MEPDG predictions for flexible pavement performance. International Journal of Pavement Engineering. 2014. 15(5-6). Pp. 392–401. DOI: 10.1080/10298436.2012.752488
5. Mogawer, W.S., Austerman, A.J., Daniel, J.S., Zhou, F., Bennert, T. Evaluation of the effects of hot mix asphalt density on mixture fatigue performance, rut performance and MEPDG distress predictions. International Journal of Pavement Engineering. 2011. 12(2). Pp. 161–175. DOI: 10.1080/10298436.2010.546857
6. Gulfam-E-Jannat, Yuan, X.X., Shehata, M. Development of regression equations for local calibration of rut and IRI as predicted by the MEPDG models for flexible pavements using Ontario's long-term PMS data. International Journal of Pavement Engineering. 2016. 17(1-2). Pp. 166–175. DOI: 10.1080/10298436.2014.973024
7. Caliendo, C. Local calibration and implementation of the mechanistic-empirical pavement design guide for flexible pavement design. Journal of Transportation Engineering. 2012. 138(3).Pp. 348–360. DOI: 10.1061/(ASCE)TE.1943-5436.0000328
8. Zhang, C., Wang, H., You, Z., Ma, B. Sensitivity analysis of longitudinal cracking on asphalt pavement using MEPDG in permafrost region. Journal of Traffic and Transportation Engineering (English Edition). 2015. 2(1). Pp. 40–47. DOI: 10.1016/j.jtte.2015.01.004
9. Li, Q., Xiao, D.X., Wang, K.C.P., Hall, K.D., Qiu, Y. Mechanistic-empirical pavement design guide (MEPDG): A bird's-eye view. Journal of Modern Transportation. 2011. 19(2). Pp. 114–133. DOI: 10.3969/j.issn.2095-087X.2011.02.007
10. Kim, S., Ceylan, H., Gopalakrishnan, K., Smadi, O. Use of pavement management information system for verification of mechanistic-empirical pavement design guide performance predictions. Transportation Research Record. 2010. 2153. Pp. 30–39. DOI: 10.3141/2153-04
11. El-Basyouny, M., Jeong, M.G. Prediction of the MEPDG asphalt concrete permanent deformation using closed form solution. International Journal of Pavement Research and Technology. 2014. 7(6). Pp. 397–404. DOI: 10.6135/ijprt.org.tw/2014
12. Cooper, S.B., Elseifi, M., Mohammad, L.N., Hassan, M. Performance and Cost-Effectiveness of Sustainable Technologies in Flexible Pavements Using the Mechanistic-Empirical Pavement Design Guide. Journal of Materials in Civil Engineering. 2012. 24(2). Pp. 239–247. DOI: 10.1061/(ASCE)MT.1943-5533.0000376
13. Solatifar, N., Kavussi, A., Abbasghorbani, M., Katicha, S.W. Development of dynamic modulus master curves of in-service asphalt layers using MEPDG models. Road Materials and Pavement Design. 2019. 20(1). Pp. 225–243. DOI: 10.1080/14680629.2017.1380688
14. Pierce, L.M., Ginger, M. Implementation of the AASHTO Mechanistic-Empirical Pavement Design Guide and Software. 2014.
15. El-Badawy, S., Bayomy, F., Awed, A. Performance of MEPDG dynamic modulus predictive models for asphalt concrete mixtures: Local calibration for Idaho. Journal of Materials in Civil Engineering. 2012. 24(11). Pp. 1412–1421. DOI: 10.1061/(ASCE)MT.1943-5533.0000518
16. Allan Reese, R. R for SAS and SPSS Users. Journal of the Royal Statistical Society: Series A (Statistics in Society). 2009. 172(3).Pp. 697–698. DOI: 10.1111/j.1467-985x.2009.00595_7.x
17. Hayes, A.F., Matthes, J. Computational procedures for probing interactions in OLS and logistic regression: SPSS and SAS implementations. Behavior Research Methods. 2009. 41(3). Pp. 924–936. DOI: 10.3758/BRM.41.3.924
18. Sandra, A.K., Sarkar, A.K. Development of a model for estimating International Roughness Index from pavement distresses. International Journal of Pavement Engineering. 2013. 14(7-8). Pp. 1–10. DOI: 10.1080/10298436.2012.703322
19. Guenther, A.B., Jiang, X., Heald, C.L., Sakulyanontvittaya, T., Duhl, T., Emmons, L.K., Wang, X. The model of emissions of gases and aerosols from nature version 2.1 (MEGAN2.1): An extended and updated framework for modeling biogenic emissions. Geoscientific Model Development. 2012. 5(22). Pp.1471–1492. DOI: 10.5194/gmd-5-1471-2012
20. Morozova, T.F., Tyanfu Khe, Petrova, Y.M. Building side area minimization at the expense of optimization the schedule of movement of workers. Magazine of civil engineering. 2011. 25(7). Pp. 1944–1949. DOI: 10.5862/mce.25.11
21. Eyring, V., Bony, S., Meehl, G.A., Senior, C.A., Stevens, B., Stouffer, R.J., Taylor, K.E. Overview of the Coupled Model Intercomparison Project Phase 6 (CMIP6) experimental design and organization. Geoscientific Model Development. 2016. 9(5). Pp. 1937–1958. DOI: 10.5194/gmd-9-1937-2016
22. Preacher, K.J., Hayes, A.F. SPSS and SAS procedures for estimating indirect effects in simple mediation models. Behavior Research Methods, Instruments, and Computers. 2004. 36(4). Pp. 717–731. DOI: 10.3758/BF03206
23. Baus, R.L., Stires, N.R. Mechanistic-Empirical Pavement Design Guide Implementation. The South Carolina Department of Transportation and the Federal Highway Administration. 2010.
24. Fediuk, R.S., Mochalov, A.V., Bituev, A.V., Zayakhanov, M.E. Structuring Behavior of Composite Materials Based on Cement, Limestone, and Acidic Ash. Inorganic Materials. 2019. 55(10). Pp. 1079–1085. DOI: 10.1134/S0020168519100042

25. Fediuk, R., Smoliakov, A., Muraviov, A. Mechanical Properties of Fiber-Reinforced Concrete Using Composite Binders. Advances in Materials Science and Engineering. 2017. DOI: 10.1155/2017/2316347
26. Zhao, Q., Cheng, P., Wang, J., Wei, Y.U. Damage prediction model for concrete pavements in seasonally frozen regions. Magazine of Civil Engineering. 2018. 84(8). DOI: 10.18720/MCE.84.6
27. Zhao, Q., Zhang, H., Fediuk, R.S., Wang, J., Fu, Q. Freeze-thaw damage model for cement pavements in seasonal frost regions. Magazine of Civil Engineering. 2021. 104(4). DOI: 10.34910/MCE.104.6

Information about authors:

***Lina Zhang**, PhD*
ORCID: https://orcid.org/0000-0002-2024-3806
E-mail: 53860470@qq.com

Dongpo He
ORCID: https://orcid.org/0000-0003-2427-1086
E-mail: hdp@nefu.edu.cn

***Qianqian Zhao,** PhD*
ORCID: https://orcid.org/0000-0002-0209-4181
E-mail: 492954791@qq.com

Received 29.09.2020. Approved after reviewing 21.07.2021. Accepted 12.08.2021.